PSFC/JA-11-14

Using laser-generated energetic protons for intertial confinement fusion radiography

Zylstra, AB.; Li, CK; Rinderknecht, HG.;
Seguin, FH.; Petrasso, RD.

June 2011

Plasma Science and Fusion Center
Massachusetts Institute of Technology
Cambridge MA 02139 USA

This work was supported in part by US DOE and LLE National Laser Users Facility (DE-FG52-07NA28059 and DE-FG03-03SF22691), LLNL (B543881 and LDRD- ER-898988), LLE (414090-G), FSC at the Univ. of Rochester (412761-G), and General Atomics (DE- AC52-06NA 27279). A. Zylstra is supported by the DOE NNSA Stewardship Science Graduate Fellowship (DE-FC52-08NA28752).

Using laser-generated energetic protons for inertial confinement fusion radiography

A. B. Zylstra,[a] C. K. Li, H. G. Rinderknecht, F. H. Séguin, and R. D. Petrasso

Plasma Science and Fusion Center, Massachusetts Institute of Technology, Cambridge, MA 02139, USA

(Dated: 16 June 2011)

The recent development of petawatt-class lasers with kilojoule-picosecond pulses, such as OMEGA EP [L. Waxer et al., Optics and photonics news, 16, 30 (2005)], provides a new diagnostic capability for study of inertial-confinement-fusion (ICF) and high-energy-density (HED) plasmas. Specifically, we discuss using petawatt OMEGA EP pulses to backlight OMEGA implosions with energetic proton beams generated through the Target Normal Sheath Acceleration (TNSA) mechanism. This allows time-resolved study of the mass distribution and electromagnetic field structures in ICF and HED plasmas. The TNSA proton backlighter offers better spatial and temporal resolution over previous techniques. We discuss target and experimental design techniques to mitigate potential problems in using TNSA backlighting to study full-energy implosions. The first proton radiographs of 60-beam spherical OMEGA implosions are presented, taken using the techniques discussed in this paper. We give sample radiographs and tips for troubleshooting failed radiography shots using TNSA backlighting. Finally, we discuss future applications of this technique at OMEGA and the NIF.

I. INTRODUCTION

A.

The Inertial Confinement Fusion (ICF) program seeks to achieve fusion ignition and positive target energy gain in the laboratory. The fundamentals of ICF were developed by Nuckolls and others[1]. The basic challenge is to compress a spherical shell of deuterium and tritium such that the central gas becomes hot and dense enough to 'spark' the reaction $\mathrm{D} + \mathrm{T} \rightarrow {}^4\mathrm{He} + \mathrm{n}$, which has $Q = 17.6$ MeV. The central spark then ignites a burn wave, which propagates through the main high-density fuel[2–5]. Currently, the ICF community is focused on upcoming ignition experiments

[a]Electronic mail: zylstra@mit.edu

at the National Ignition Facility (NIF)[6].

Understanding target and hohlraum physics is crucial to achieving ignition at the NIF. A varied suite of diagnostics has been developed for the NIF for the tuning campaign. However, fundamental physics is easily studied at smaller scale facilities, such as OMEGA and OMEGA EP at the University of Rochester[7,8].

B. Previous techniques

One successful technique for ICF physics studies has been radiography, using either x-rays[9,10] or charged particles, which will be the focus of this paper. Several years ago a fusion-based charged particle backlighter was developed at OMEGA[11]. Primarily this technique uses 3 and 15 MeV protons (from DD and D^3He fusion), produced in a 80-130ps burn with a typical source size of 40-50μm FWHM. This technique has been successfully used to study direct-drive implosions[12–14], indirect-drive implosions[15–17], and electromagnetic fields in HED plasmas[18–22].

C. Energetic proton production

It is well known that the interaction of a high-intensity laser with matter can create energetic electrons and ions[23,24]. Relevant to this work is the Target Normal Sheath Acceleration (TNSA) mechanism at order 10^{19} W/cm^2. During the initial laser interaction with a high-Z solid target electrons are accelerated to high energy, and propagate away from the target at nearly the speed of light, c. This sets up strong 'sheath' electric fields, which can accelerate ions to high energy. Hydrocarbon contaminants on the target are known to cause the production of energetic protons, up to 60 MeV. Ion acceleration mechanisms, including TNSA, have been extensively studied experimentally[25–44] and computationally[45–48]. Other proposed applications for this technique include compact medical and research accelerators, and proton fast ignition[49].

D. Challenges and benefits of TNSA backlighting

An obvious use of these sheath-generated proton beams is as a backlighter for ICF and HED plasmas. This has been proposed and used in the literature[50–54], and recently in experiments on OMEGA EP only[55–57]. However, backlighting full-scale implosions at OMEGA or the NIF comes with a unique set of challenges and benefits for TNSA proton backlighting.

These challenges include designing the backlighter to ensure an adequate fluence and energy of backlighting pro-

tons. This requires compensating for several effects, such as x-ray crosstalk, return current, and preplasma from the implosion[58]. The beam divergence, magnification required, and desired radiography time window present an experimental optimization problem.

Benefits of TNSA proton backlighting over previous proton backlighting, i.e. with fusion-generated protons, are better temporal resolution (∼10ps versus ∼100ps), better spatial resolution (∼10μm[36] versus 40-50μm), and the ability to radiograph at several time steps during one implosion. The fusion backlighter offers better energy resolution and spatial uniformity than the TNSA backlighter; which technique is better will depend on the experiment.

This work focuses on solutions to the unique challenges in using TNSA backlighting for 60-beam OMEGA implosions, and presents the first radiographs of such implosions. The paper is organized as follows: Section II presents an overview of the facilities and experiment; Section III details the specifics of our backlighter design; Section IV discusses the optimzation of beam divergence, magnification, and timing; Section V discusses the design of radiochromic film packs for proton measurements; Section VI presents the first results of this method; Section VII gives some characteristics of common failures for troubleshooting TNSA backlighting; finally the paper is concluded in Sections VIII and IX.

II. EXPERIMENTAL OVERVIEW

The OMEGA facility[7] is a 60-beam frequency-tripled Nd:glass laser, which produces up to 30kJ UV in 1 to several ns pulses. The OMEGA EP petawatt laser facility[8] has two 'long pulse' beams (order ns), and two 'short pulse' beams (1-100ps pulses). One of the short pulse beams can be transferred to the OMEGA target chamber for joint shot operations. Currently, the system is capable of ∼300J UV in 1ps or ∼1kJ UV in 10ps.

In this experiment all 60 OMEGA beams drive the subject spherical capsule implosion. A top-level schematic of the experiment is shown in Fig. 1. The target is a 20-40μm thick CH shell of outer diameter 860μm filled with ^{4}He gas at 18atm. The OMEGA pulse shape is a 3.5ns 17kJ 'shock ignition' pulse[59] using the SSD driver and SG4 phase plates, as the ultimate physics goal is to study the shock propagation in the imploded capsule. The capsule drive pulse is started several ns before the backlighter is fired, as the most interesting physics occurs when the shock is launched, as well as near 'burn' and stagnation. The actual backlighter foil used was 10μm thick Au. We used a 1ps 300J short-pulse beam for TNSA backlighting, with a focal spot size $\sim 40\mu$m in diameter for an intensity $\approx 2 \times 10^{19}$ W/cm^2.

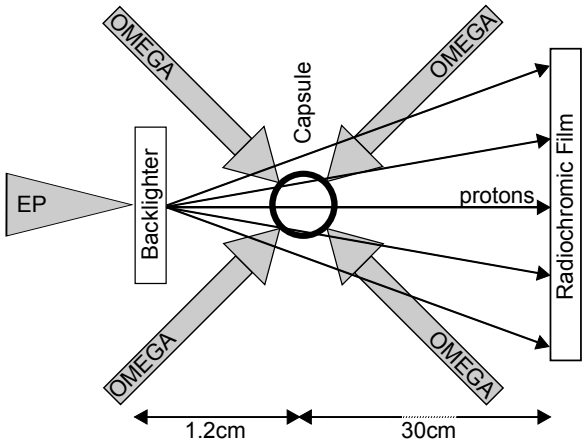

FIG. 1. Top-level schematic of the experiment. Sixty OMEGA beams drive a spherical implosion, which is backlit by the EP laser-generated protons and imaged on a radiochromic film detector.

III. BACKLIGHTER DESIGN

As listed in the introduction, there are three main mechanisms for backlighter performance degradation in this environment:

A. Preplasma

It is known that any prepulse on the proton-generating laser beam can create a 'preplasma' at the target, which dramatically reduces the backlighter performance. In this experiment the subject capsule is imploded via sixty OMEGA beams via ablation pressure. The ablated mass is ejected outwards to large radii, forming a large coronal plasma around the implosion. Since the capsule drive starts several ns before backlighting, the coronal plasma can reach the backlighter. In a simple geometry, Fig. 2, the coronal plasma flows around the backlighter foil and can impede the short-pulse beam propagation to the solid foil surface. This has the same effect as preplasma: the conversion efficiency from laser energy to energetic protons is greatly reduced. The backlighter must therefore be designed to impede the coronal plasma flow so that it does not interact with the short-pulse beam propagation.

B. X-ray crosstalk

X-ray imaging of capsule implosions can show that the capsule emits x-rays during the drive. These x-rays are emitted isotropically, so some fraction will be incident on the backlighter foil. This is shown schematically in Fig. 3. Since the backlighter foil is high Z the x-rays will efficienctly heat it, which can create some preplasma on the back

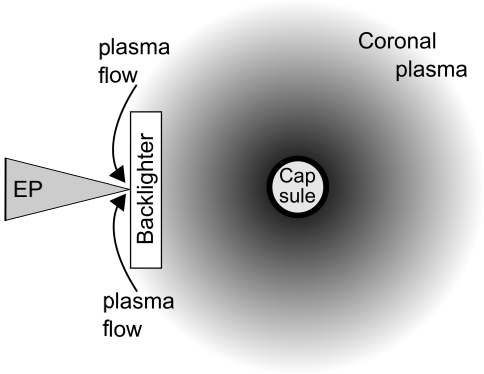

FIG. 2. A coronal plasma forms around an imploding capsule due to ablation blowoff from the OMEGA drive. The coronal plasma can flow around the backlighter foil to reach where the short pulse beam propagates.

surface ∼ns before the short-pulse beam is incident on the foil. This would be a similar effect to a prepulse on the short-pulse beam, or interference by coronal plasma. To mitigate this effect the backlighter foil must be shielded from 'crosstalk' with the capsule.

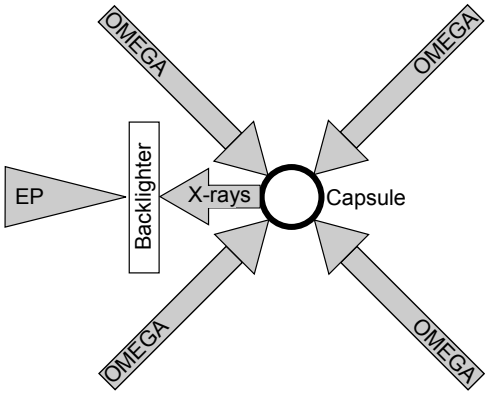

FIG. 3. 60 OMEGA beams drive the capsule implosion. X-rays from the capsule can preheat the backlighter foil, which will reduce the backlighter performance.

C. Return current

In the TNSA mechanism fast electrons escape from the backlighter foil due to the high-intensity laser-matter interaction, as shown in Fig. 4. This sets up a strong electric sheath field, which accelerates the protons of interest for TNSA backlighting. If, for example, a shield foil is placed in front of the backlighter foil to shield from x-ray crosstalk (previous section), then there is a potential for the fast electrons to form a return current back to the backlighter foil. This would neutralize the acceleration sheath field, and reduce the backlighter proton performance.

Therefore, we must have a total backlighter size greater than the scale length $\ell = c\tau$, where τ is the laser pulse

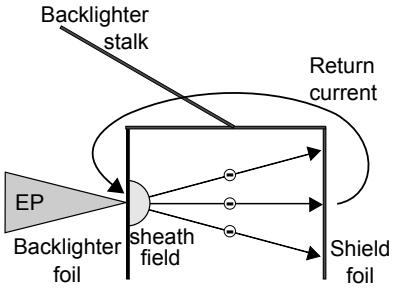

FIG. 4. If there is a pathway for fast electrons to form a return current to the backlighter foil within the backlighter pulse, then the sheath field can be neutralized.

length, and the electrons are ultra-relativistic ($v \approx c$). With a 1ps pulse $\ell \sim 0.3$mm, and at $\tau = 10$ps the scale length $\ell \sim 3$mm. Since typical backlighter sizes are of order mm, this is a design concern for 10ps pulses but not 1ps.

D. Resulting Design

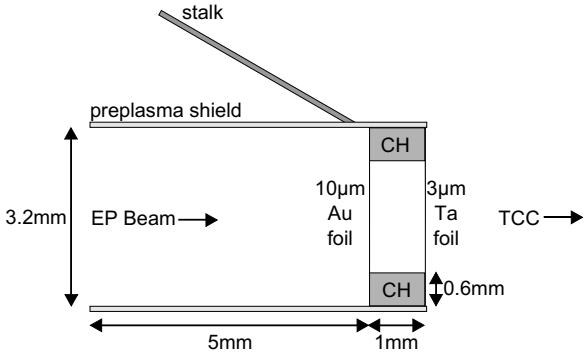

FIG. 5. Backlighter design used in these experiments. Shown is a cross-section, where the design has cylindrical symmetry around the central axis (except for the target positioner stalk).

A backlighter for joint OMEGA and EP TNSA radiography has been designed to mitigate these issues. A schematic is shown in Fig. 5, and fabricated backlighters are shown in Fig. 6.

The 10μm Au foil is the actual backlighter foil target. The foil is glued to a thin CH washer. On the other end of the washer, we glue a 3μm Ta foil as a x-ray cross-talk shield. The washer is encased in a thin brass cylindrical shell, which forms a shield to impede coronal plasma flow to the backlighter foil. As shown in Fig. 5 the EP beam comes in from the left, and TCC is to the right. As a 1ps pulse is used in these experiments, there is no potential for return current issues due to the scale lengths of this backlighter design.

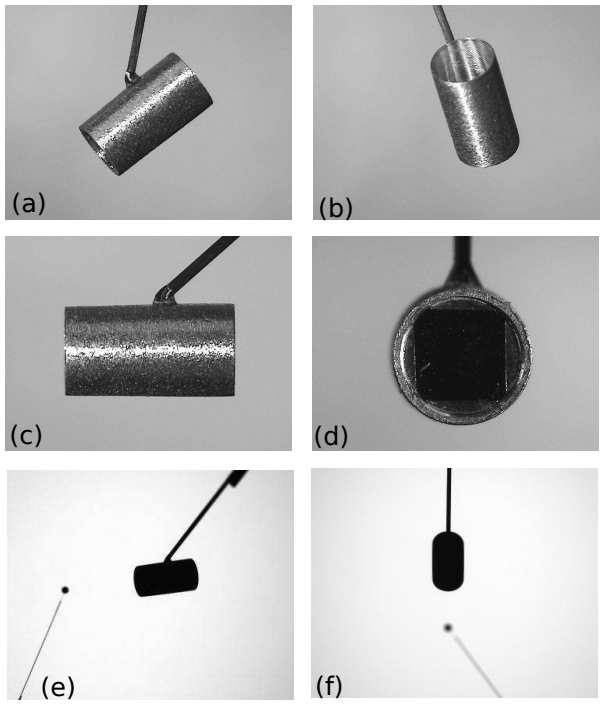

FIG. 6. Images of fabricated and fielded backlighters. From top left: (a,b) two isometric views of a fabricated backlighter, (c) side-on view of backlighter, (d) view from TCC of backlighter, (e,f) shadowgraphs of pre-shot backlighter and capsule in OMEGA target chamber.

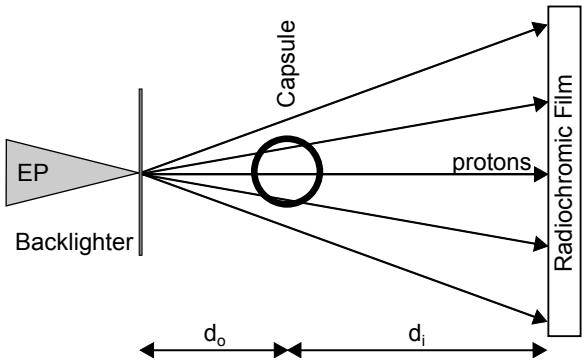

FIG. 7. The radiography time-of-flight, magnification, and EP backlighter performance depend on the backlighter-object distance (d_o) and object-film distance (d_i).

IV. EXPERIMENTAL OPTIMIZATION

The experimental configuration, i.e. separation between backlighter, subject, and imaging plane, must be adjusted to optimize the backlighter performance, magnification, and radiography timing. We call the backlighter-capsule distance d_o and the capsule-film distance d_i, as shown in Fig. 7.

The TNSA-generated proton beam has a cone-shaped emission, so with a given beam intensity a larger d_i results in less fluence on the detector. In joint radiography experiments we observe that the film pack performs well for

$d_i \sim 30$cm.

Additionally, the magnification is

$$M = \frac{d_i + d_o}{d_o} = 1 + \frac{d_i}{d_o} \tag{1}$$

Since the interesting physics in a capsule implosions happens at small radii, $\leq 200\mu$m, the magnification must be at least 25 for detectable features. With $d_i \approx 30$cm, this constrains $d_o \leq 1.25$cm. Depending on the experimental goals a higher magnification may be desirable.

Finally, the radiography time-of-flight depends on the choice of d_o. Since the TNSA mechanism produces a falling exponential distribution with proton energy, we can simultaneously use low- (several MeV) and high- (several tens of MeV) energy protons to backlight the implosion. All protons are born essentially simultaneously, within 1-10ps depending on the high-intensity laser pulse length, so each proton energy backlights the implosion at a time

$$t = \tau + d_o/v_p \tag{2}$$

where τ is the short-pulse laser delay, and $v_p = v_p(E)$ is the proton velocity. So the time window radiographed in one shot is

$$\delta t = d_o \left(\frac{1}{v_{p,min}} - \frac{1}{v_{p,max}} \right) \tag{3}$$

where $v_{p,min}$ and $v_{p,max}$ are respectively the minimum and maximum energies for which usable radiographs are obtained. Ideally this is ≥ 150ps to allow radiography of a large total time window of the implosion physics within one shot day. This is easily achievable with the film pack design in this paper for $d_o = 1.2$cm, as will be shown in the next section.

V. FILM PACK DESIGN

The film pack used in these experiments is shown in Fig. 8. Protons from the backlighter are incident from the left. A series of Al or Ta filters and Gafchromic® HD-810 radiochromic films are interleaved. The filter pack size is 10cm × 10cm. Each filter is measured with a micrometer since the thickness tolerance is generally 10% (standard

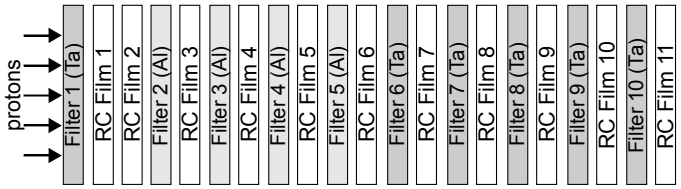

FIG. 8. Radiochromic (RC) film pack design for detection of proton radiographs. The pack consists of interleaved filters (Al or Ta) and films.

filter stock from Goodfellow®). Each filter's material and measured thickness is listed in Table I.

TABLE I. Film pack filter materials and thicknesses

Filter	Material	Thickness (μm)
1	Ta	42
2	Al	29
3	Al	106
4	Al	205
5	Al	480
6	Ta	390
7	Ta	407
8	Ta	534
9	Ta	1027
10	Ta	1026

With known filter thicknesses and composition information on the HD-810 film, we calculate the proton energy that each film is primarily sensitive to, ϵ, using SRIM[60] calculated stopping powers. This is done by calculating the deposited energy per incident proton energy for initial proton energies from 0 to 60 MeV. This is shown for a specific film, 5, in Fig. 9.

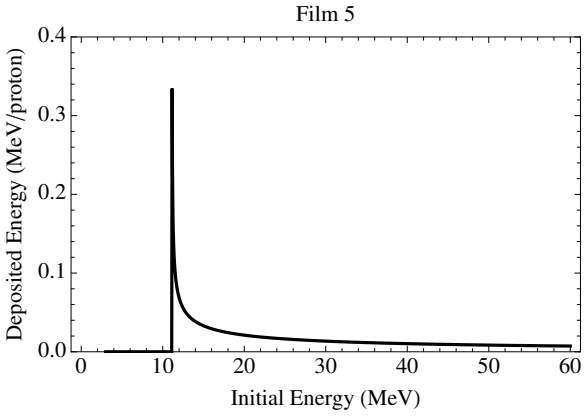

FIG. 9. Sensitivity versus initial proton energy for film 5, chosen as an example of typical behavior.

With ϵ we can also calculate a time-of-flight for each film, which corresponds to when that radiograph is taken. This information is given in Table II.

TABLE II. Film pack proton energy of maximum sensitivity, ϵ, and time-of-flight (TOF) to the subject implosion d_o/v_p for $d_o = 1.2$cm.

Film	ϵ (MeV)	TOF (ns)
1	3.8	0.64
2	5.2	0.54
3	6.6	0.48
4	8.6	0.42
5	11.2	0.37
6	15.3	0.32
7	22.8	0.26
8	29.4	0.23
9	36.8	0.21
10	48.4	0.18
11	58.4	0.17

In future experiments, the magnification will be increased by decreasing d_o. In this case it is useful to show how the sample timing changes with d_o. The TOF curve for arbitrary proton energy, with chosen film energies marked, is shown in Fig. 10 for $d_o = 0.6, 0.9, 1.2$cm.

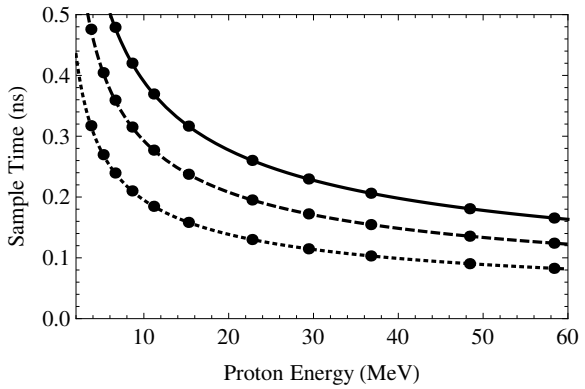

FIG. 10. Time-of-flight curves for $d_o = 0.6$cm (dotted line), $= 0.9$cm (dashed line), and $= 1.2$cm (solid line). The points mark specific film energies (see Table II).

Another film pack consideration is the high-energy tail to the film sensitivity, as can be seen in Fig. 9. The peak sensitivity is narrow due to the Bragg peak, but the integrated tail as shown for a single film sensitivity is significant. However, in the TNSA proton production mechanism there is a falling exponential energy distribution, which will tend to suppress the high-energy tail of the sensitivity. We thus fold an approximate distribution with the sensitivities calculated for each film, which is shown in Fig. 11. In future shots the last 2-3 films will be replaced by higher sensitivity Gafchromic® MD-V2-55 films.

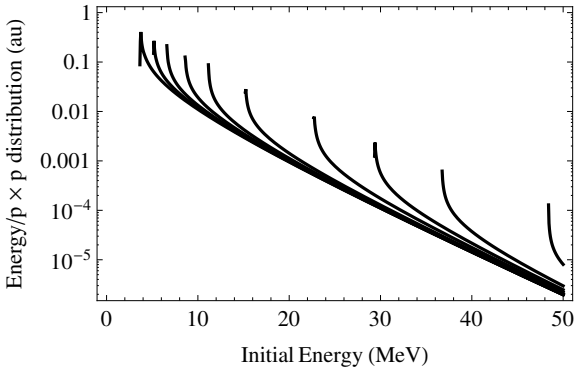

FIG. 11. RC film sensitivity, as energy deposited per proton, folded with an assumed exponential proton distribution and plotted versus initial energy. All eleven films are shown, from film 1 to 11 from left to right.

In future experiments the proton distribution can be measured by taking a backlighter-only shot. With a microdensitometer or optical microscope to measure the film optical density and known film response[61], exact proton fluence can be calculated using this sensitivity method.

VI. RESULTS

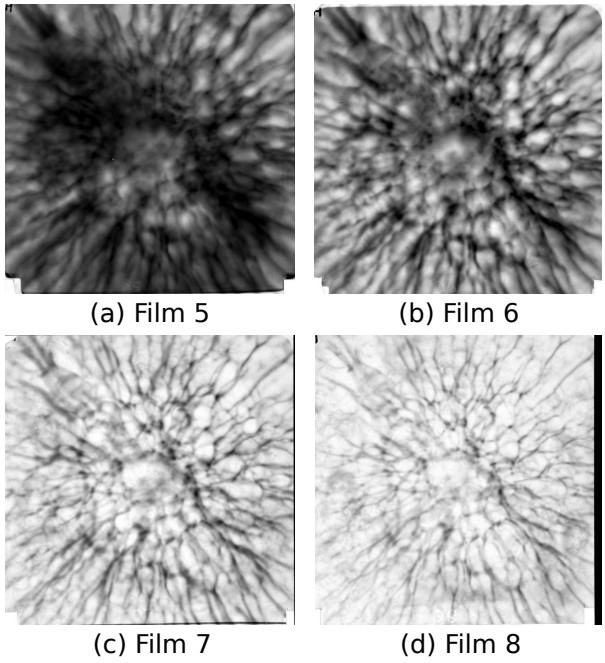

FIG. 12. A series of radiographs of the filametary field structure around an imploded capsule, OMEGA shot 61250. The backlighting protons are produced 3.53ns after the capsule drive begins. For film energies and timing, see Table II.

Using the techniques outlined in the previous sections, a series of radiographs was taken of the filamentary electromagnetic field structure around an imploded capsule. Four sequential films are shown in Fig. 12. This data was taken

with the film pack configured as in Section V, with a 17kJ shock ignition pulse (FIS3601P) driving the capsule with all 60 OMEGA beams, and a 300J 1ps EP pulse generating the backlighting protons, using the backlighter design in Section III. For this shot $d_o = 1.2$cm and d_i=30cm, so the magnification is 26 and the RC film field of view is thus 3.8mm at the target plane.

VII. DIAGNOSING FAILED RADIOGRAPHY

If a radiography shot fails it is important to troubleshoot the failure with the smallest number of additional shots and least amount of time, given the experimental constraints at facilities like OMEGA and OMEGA EP. On a typical joint shot day, a PI can only expect 6 ± 1 radiography shots. Therefore we give tips for recognizing two common failures on the basis of our experience backlighting implosions.

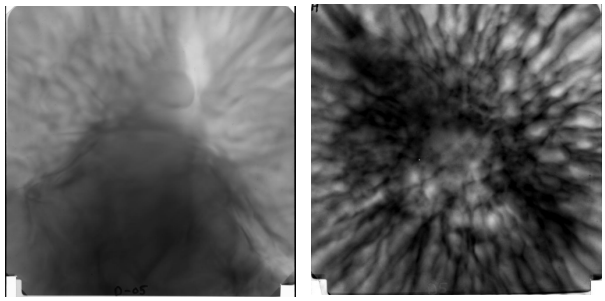

(a) Film 5, Shot 59141 (b) Film 5, Shot 61250

FIG. 13. Comparison of 60-beam OMEGA radiographs using backlighters without (left) and with (right) a preplasma shield, as discussed in Section III.

The preplasma issue, as discussed in Section III A and Fig. 2, can seriously degrade the backlighter performance. When the coronal plasma interferes with the EP beam propagation the proton beam emission is more diffuse, and the highest energy proton produced is low (10-20 MeV instead of ~ 50). In particular, we have observed diffuse large-scale structures. This is shown in Fig. 13. The left image shows a radiograph where the backlighter did not have a preplasma shield, and the right image did have a shield as detailed in Section III. On the left we can see some of the filametary structure in the top left and top right, but most of the image is dominated by a large diffuse structure resulting from the preplasma. On the right, with a preplasma shield, we obtain a radiograph of the entire implosion.

If the film pack is too far away (d_i is too large) then the TNSA proton beam divergence can mean that the fluence on the detector is too low. If this is the case, then it affects the high-energy films first due to the exponential distribution. Thus a low proton energy cutoff ($10 - 20$ MeV instead of ~ 50) but sharp radiographs at low energy results from

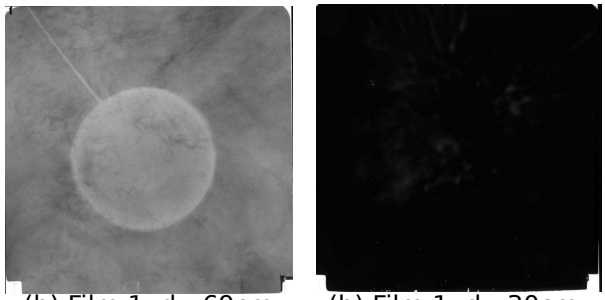

FIG. 14. Comparison of lowest-energy radiographs when d_i is too large (left) and when d_i is optimized (right).

d_i being too large. This is shown in Fig. 14. On the left is a radiograph of an unimploded capsule with the lowest energy film at $d_i = 69$cm. The higher energy films did not have visible radiographs. On the right is the same film on a shot with $d_i = 30$cm, and the higher fluence has almost saturated the film. At higher energies for shot 61250 excellent radiographs are obtained (see Fig. 12).

VIII. CONCLUSIONS

Petawatt-class lasers with kilojoule-picosecond pulses offer new opportunities for ICF and HEDP radiography, including using the TNSA energetic proton production mechanism for proton backlighting. This technique offers better temporal and spatial resolution over previous fusion-based proton backlighters, and offers a wide range of proton energies which is beneficial for mapping out field structures in ICF and HEDP plasmas. We present the first results of using TNSA proton backlighting to image 60-beam OMEGA implosions. In such experiments there are several challenges to using the TNSA mechanism to generate backlighting protons, such as avoiding preplasma, crosstalk, return current, and optimizing the experimental configuration to achieve the desired magnification, timing, and fluence at the radiochromic film detector. This work presents solutions to this issues, which will allow future joint OMEGA and OMEGA EP experiments to use TNSA backlighting to study ICF and HEDP physics.

IX. FUTURE WORK

This technique will be applied to study shock propagation in shock ignition implosions at OMEGA, in particular using high-energy protons to probe the electromagnetic field structure at the shock front. The improved spatial and temporal resolution will also be used to study electromagnetic fields in hohlraums around the laser entrance hole

(LEH) and at plasma bubbles formed at the wall, expanding on previous efforts[15–17].

The future NIF Advanced Radiographic Capability (ARC)[62] will allow the study of full-scale NIF experiments using a petawatt-class laser. Radiography using NIF ARC will be at similar drive conditions to OMEGA EP (kilojoule-picosecond pulses), and with similar challenges to those discussed in this work. NIF ARC proton radiography will provide an important diagnostic for electromagnetic field structures in megajoule indirect- and direct- drive implosions. It will be important to transfer experience with TNSA backlighting from full-scale joint OMEGA experiments, as discussed in this work, to future radiography using ARC on the NIF.

ACKNOWLEDGMENTS

The authors would like thank the engineering and operations staff at the OMEGA and OMEGA EP facilities for their support, and C. Stoeckl for short-pulse beam timing assistance. This work was supported in part by US DOE and LLE National Laser Users Facility (DE-FG52-07NA28059 and DE-FG03-03SF22691), LLNL (B543881 and LDRD-ER-898988), LLE (414090-G), FSC at the Univ. of Rochester (412761-G), and General Atomics (DE- AC52-06NA 27279). A. Zylstra is supported by the DOE NNSA Stewardship Science Graduate Fellowship (DE-FC52-08NA28752).

[1] J. Nuckolls, L. Wood, A. Thiessen, and G. Zimmerman, Nature **239**, 139 (1972).

[2] J. Lindl, R. McCrory, and E. Campbell, Physics Today **45**, 32 (1992).

[3] J. Lindl, Physics of Plasmas **2**, 3933 (1995).

[4] S. Haan, S. Pollaine, J. Lindl, L. Suter, R. Berger, L. Powers, W. Alley, P. Amendt, J. Futterman, W. Levedahl, M. Rosen, D. Rowley, R. Sacks, A. Shestakov, G. Strobel, M. Tabak, S. Weber, and G. Zimmerman, Physics of Plasmas **2**, 2480 (1995).

[5] S. Atzeni and J. Meyer-ter Vehn, *The physics of inertial fusion* (Clarendon Pr., 2004).

[6] G. Miller, E. Moses, and C. Wuest, Nuclear fusion **44**, S228 (2004).

[7] T. Boehly, D. Brown, R. Craxton, R. Keck, J. Knauer, J. Kelly, T. Kessler, S. Kumpan, S. Loucks, S. Letzring, F. Marshall, R. McCrory, S. Morse, W. Seka, J. Soures, and C. Verdon, Optics communications **133**, 495 (1997).

[8] L. Waxer, D. Maywar, J. Kelly, T. Kessler, B. Kruschwitz, S. Loucks, R. McCrory, D. Meyerhofer, S. Morse, C. Stoeckl, and J. Zuegel, Optics and photonics news **16**, 30 (2005).

[9] R. Tommasini, A. MacPhee, D. Hey, T. Ma, C. Chen, N. Izumi, W. Unites, A. MacKinnon, S. Hatchett, B. Remington, H. Park, P. Springer, J. Koch, O. Landen, J. Seely, G. Holland, and L. Hudson, Review of Scientific Instruments **79**, 10E901 (2008).

[10] F. Marshall, P. McKenty, J. Delettrez, R. Epstein, J. Knauer, V. Smalyuk, J. Frenje, C. Li, R. Petrasso, F. Séguin, and R. Mancini, Physical review letters **102**, 185004 (2009).

[11] C. Li, F. Seguin, J. Frenje, J. Rygg, R. Petrasso, R. Town, P. Amendt, S. Hatchett, O. Landen, A. Mackinnon, P. Patel, V. Smalyuk, J. Knauer, T. Sangster, and C. Stoeckl, Review of scientific instruments **77**, 10E725 (2006).

[12]C. Li, F. Séguin, J. Rygg, J. Frenje, M. Manuel, R. Petrasso, R. Betti, J. Delettrez, J. Knauer, F. Marshall, D. Meyerhofer, D. Shvarts, V. Smalyuk, C. Stoeckl, O. Landen, R. Town, C. Back, and J. Kilkenny, Physical review letters **100**, 225001 (2008).

[13]J. Rygg, F. Séguin, C. Li, J. Frenje, M. Manuel, R. Petrasso, R. Betti, J. Delettrez, O. Gotchev, J. Knauer, D. Meyerhofer, F. Marshall, C. Stoeckl, and W. Theobald, Science **319**, 1223 (2008).

[14]C. Li, F. Séguin, J. Frenje, M. Manuel, R. Petrasso, V. Smalyuk, R. Betti, J. Delettrez, J. Knauer, F. Marshall, D. Meyerhofer, D. Shvarts, C. Stoeckl, W. Theobald, J. Rygg, O. Landen, R. Town, P. Amendt, C. Back, and J. Kilkenny, Plasma Physics and Controlled Fusion **51**, 014003 (2009).

[15]C. Li, F. Séguin, J. Frenje, R. Petrasso, P. Amendt, R. Town, O. Landen, J. Rygg, R. Betti, J. Knauer, D. Meyerhofer, J. Soures, C. Back, J. Kilkenny, and A. Nikroo, Physical review letters **102**, 205001 (2009).

[16]C. Li, F. Séguin, J. Frenje, M. Rosenberg, R. Petrasso, P. Amendt, J. Koch, O. Landen, H. Park, H. Robey, R. Town, A. Casner, F. Philippe, R. Betti, J. Knauer, D. Meyerhofer, C. Back, J. Kilkenny, and A. Nikroo, Science **327**, 1231 (2010).

[17]C. Li, F. Séguin, J. Frenje, M. Rosenberg, A. Zylstra, R. Petrasso, P. Amendt, J. Koch, O. Landen, H. Park, H. Robey, R. Town, A. Casner, F. Philippe, R. Betti, J. Knauer, D. Meyerhofer, C. Back, J. Kilkenny, and A. Nikroo, Plasma Physics and Controlled Fusion **52**, 124027 (2010).

[18]C. Li, F. Séguin, J. Frenje, J. Rygg, R. Petrasso, R. Town, P. Amendt, S. Hatchett, O. Landen, A. Mackinnon, P. Patel, V. Smalyuk, T. Sangster, and J. Knauer, Physical review letters **97**, 135003 (2006).

[19]C. Li, F. Séguin, J. Frenje, J. Rygg, R. Petrasso, R. Town, P. Amendt, S. Hatchett, O. Landen, A. Mackinnon, P. Patel, M. Tabak, J. Knauer, T. Sangster, and V. Smalyuk, Physical review letters **99**, 15001 (2007).

[20]C. Li, F. Séguin, J. Frenje, J. Rygg, R. Petrasso, R. Town, O. Landen, J. Knauer, and V. Smalyuk, Physical review letters **99**, 55001 (2007).

[21]R. Petrasso, C. Li, F. Seguin, J. Rygg, J. Frenje, R. Betti, J. Knauer, D. Meyerhofer, P. Amendt, D. Froula, O. Landen, P. Patel, J. Ross, and R. Town, Physical review letters **103**, 85001 (2009).

[22]C. Li, F. Séguin, J. Frenje, M. Manuel, D. Casey, N. Sinenian, R. Petrasso, P. Amendt, O. Landen, J. Rygg, R. Town, R. Betti, J. Delettrez, J. Knauer, F. Marshall, D. Meyerhofer, T. Sangster, D. Shvarts, V. Smalyuk, J. Soures, C. Back, J. Kilkenny, and A. Nikroo, Physics of Plasmas **16**, 056304 (2009).

[23]J. Badziak, Opto-Electronics Review **15**, 1 (2007).

[24]P. Norreys, Nature Photonics **3**, 423 (2009).

[25]A. Fews, P. Norreys, F. Beg, A. Bell, A. Dangor, C. Danson, P. Lee, and S. Rose, Physical review letters **73**, 1801 (1994).

[26]S. Hatchett, C. Brown, T. Cowan, E. Henry, J. Johnson, M. Key, J. Koch, A. Langdon, B. Lasinski, R. Lee, A. Mackinnon, D. Pennington, M. Perry, T. Phillips, M. Roth, T. Sangster, M. Singh, R. Snavely, M. Stoyer, S. Wilks, and K. Yasuike, Physics of Plasmas **7**, 2076 (2000).

[27]K. Krushelnick, E. Clark, M. Zepf, J. Davies, F. Beg, A. Machacek, M. Santala, M. Tatarakis, I. Watts, P. Norreys, and A. Dangor, Physics of Plasmas **7**, 2055 (2000).

[28]A. Maksimchuk, S. Gu, K. Flippo, D. Umstadter, and V. Bychenkov, Physical Review Letters **84**, 4108 (2000).

[29]R. Snavely, M. Key, S. Hatchett, T. Cowan, M. Roth, T. Phillips, M. Stoyer, E. Henry, T. Sangster, M. Singh, S. Wilks, A. MacKinnon,

A. Offenberger, D. Pennington, K. Yasuike, A. Langdon, B. Lasinski, J. Johnson, M. Perry, and E. Campbell, Physical Review Letters **85**, 2945 (2000).

[30]A. Mackinnon, M. Borghesi, S. Hatchett, M. Key, P. Patel, H. Campbell, A. Schiavi, R. Snavely, S. Wilks, and O. Willi, Physical Review Letters **86**, 1769 (2001).

[31]A. Mackinnon, Y. Sentoku, P. Patel, D. Price, S. Hatchett, M. Key, C. Andersen, R. Snavely, and R. Freeman, Physical review letters **88**, 215006 (2002).

[32]M. Roth, A. Blazevic, M. Geissel, T. Schlegel, T. Cowan, M. Allen, J. Gauthier, P. Audebert, J. Fuchs, J. Meyer-ter Vehn, M. Hegelich, S. Karsch, and A. Pukhov, Physical Review Special Topics-Accelerators and Beams **5**, 61301 (2002).

[33]M. Roth, M. Allen, P. Audebert, A. Blazevic, E. Brambrink, T. Cowan, J. Fuchs, J. Gauthier, M. Geißel, M. Hegelich, S. Karsch, J. Meyer-ter Vehn, T. Ruhl, H aand Schlegel, and R. Stephens, Plasma physics and controlled fusion **44**, B99 (2002).

[34]M. Zepf, E. Clark, F. Beg, R. Clarke, A. Dangor, A. Gopal, K. Krushelnick, P. Norreys, M. Tatarakis, U. Wagner, and M. Wei, Physical review letters **90**, 64801 (2003).

[35]M. Allen, P. Patel, A. Mackinnon, D. Price, S. Wilks, and E. Morse, Physical review letters **93**, 265004 (2004).

[36]M. Borghesi, A. J. Mackinnon, D. H. Campbell, D. G. Hicks, S. Kar, P. K. Patel, D. Price, L. Romagnani, A. Schiavi, and O. Willi, Phys. Rev. Lett. **92**, 055003 (2004).

[37]J. Fuchs, P. Antici, E. D'Humieres, E. Lefebvre, M. Borghesi, E. Brambrink, C. Cecchetti, M. Kaluza, V. Malka, M. Manclossi, S. Meyroneinc, P. Mora, J. Schreiber, T. Toncian, H. Pepin, and P. Audebert, Nature Physics **2**, 48 (2005).

[38]J. Fuchs, Y. Sentoku, S. Karsch, J. Cobble, P. Audebert, A. Kemp, A. Nikroo, P. Antici, E. Brambrink, A. Blazevic, E. Campbell, J. Fernandez, J. Gauthier, M. Geissel, M. Hegelich, H. Pepin, H. Popescu, N. Renard-LeGalloudec, M. Roth, J. Schreiber, R. Stephens, and T. Cowan, Physical review letters **94**, 45004 (2005).

[39]L. Romagnani, J. Fuchs, M. Borghesi, P. Antici, P. Audebert, F. Ceccherini, T. Cowan, T. Grismayer, S. Kar, A. Macchi, P. Mora, G. Pretzler, A. Schiavi, T. Toncian, and O. Willi, Physical review letters **95**, 195001 (2005).

[40]M. Borghesi, J. Fuchs, S. Bulanov, A. Mackinnon, P. Patel, and M. Roth, Fusion science and technology **49**, 412 (2006).

[41]D. Neely, P. Foster, A. Robinson, F. Lindau, O. Lundh, A. Persson, C. Wahlstr
"om, and P. McKenna, Applied physics letters **89**, 021502 (2006).

[42]S. Kar, K. Markey, P. T. Simpson, C. Bellei, J. S. Green, S. R. Nagel, S. Kneip, D. C. Carroll, B. Dromey, L. Willingale, E. L. Clark, P. McKenna, Z. Najmudin, K. Krushelnick, P. Norreys, R. J. Clarke, D. Neely, M. Borghesi, and M. Zepf, Phys. Rev. Lett. **100**, 105004 (2008).

[43]K. Flippo, T. Bartal, F. Beg, S. Chawla, J. Cobble, S. Gaillard, D. Hey, A. MacKinnon, A. MacPhee, P. Nilson, D. Offermann, S. Le Pape, and M. Schmitt, in *Journal of Physics: Conference Series*, Vol. 244 (2010) p. 022033.

[44]L. Willingale, G. M. Petrov, A. Maksimchuk, J. Davis, R. R. Freeman, T. Matsuoka, C. D. Murphy, V. M. Ovchinnikov, L. V. Woerkom, and K. Krushelnick, Plasma Physics and Controlled Fusion **53**, 014011 (2011).

[45]A. Pukhov, Physical Review Letters **86**, 3562 (2001).

[46]S. Wilks, A. Langdon, T. Cowan, M. Roth, M. Singh, S. Hatchett, M. Key, D. Pennington, A. MacKinnon, and R. Snavely, Physics of Plasmas **8**, 542 (2001).

[47]Y. Sentoku, T. Cowan, A. Kemp, and H. Ruhl, Physics of Plasmas **10**, 2009 (2003).

[48]G. M. Petrov, L. Willingale, J. Davis, T. Petrova, A. Maksimchuk, and K. Krushelnick, Physics of Plasmas **17**, 103111 (2010).

[49]M. Roth, T. Cowan, M. Key, S. Hatchett, C. Brown, W. Fountain, J. Johnson, D. Pennington, R. Snavely, S. Wilks, K. Yasuike, H. Ruhl, F. Pegoraro, S. Bulanov, E. Campbell, M. Perry, and H. Powell, Physical Review Letters **86**, 436 (2001).

[50]E. Clark, K. Krushelnick, J. Davies, M. Zepf, M. Tatarakis, F. Beg, A. Machacek, P. Norreys, M. Santala, I. Watts, and A. Dangor, Physical Review Letters **84**, 670 (2000).

[51]M. Borghesi, A. Schiavi, D. Campbell, M. Haines, O. Willi, A. MacKinnon, L. Gizzi, M. Galimberti, R. Clarke, and H. Ruhl, Plasma physics and controlled fusion **43**, A267 (2001).

[52]M. Borghesi, D. Campbell, A. Schiavi, M. Haines, O. Willi, A. MacKinnon, P. Patel, L. Gizzi, M. Galimberti, R. Clarke, F. Pegoraro, H. Ruhl, and S. Bulanov, Physics of Plasmas **9**, 2214 (2002).

[53]J. Cobble, R. Johnson, T. Cowan, N. Renard-Le Galloudec, and M. Allen, Journal of applied physics **92**, 1775 (2002).

[54]A. J. Mackinnon, P. K. Patel, M. Borghesi, R. C. Clarke, R. R. Freeman, H. Habara, S. P. Hatchett, D. Hey, D. G. Hicks, S. Kar, M. H. Key, J. A. King, K. Lancaster, D. Neely, A. Nikkro, P. A. Norreys, M. M. Notley, T. W. Phillips, L. Romagnani, R. A. Snavely, R. B. Stephens, and R. P. J. Town, Phys. Rev. Lett. **97**, 045001 (2006).

[55]L. Willingale, A. Thomas, P. Nilson, M. Kaluza, S. Bandyopadhyay, A. Dangor, R. Evans, P. Fernandes, M. Haines, C. Kamperidis, R. Kingham, S. Minardi, M. Notley, C. Ridgers, W. Rozmus, M. Sherlock, M. Tatarakis, M. Wei, Z. Najmudin, and K. Krushelnick, Physical review letters **105**, 95001 (2010).

[56]L. Willingale, P. Nilson, M. Kaluza, A. Dangor, R. Evans, P. Fernandes, M. Haines, C. Kamperidis, R. Kingham, C. Ridgers, M. Sherlock, A. Thomas, M. Wei, Z. Najmudin, K. Krushelnick, S. Bandyopadhyay, M. Notely, S. Minardi, M. Tatarakis, and W. Rozmus, Physics of Plasmas **17**, 043104 (2010).

[57]L. Willingale, P. Nilson, A. Thomas, J. Cobble, R. Craxton, A. Maksimchuk, P. Norreys, T. Sangster, R. Scott, C. Stoeckl, C. Zulick, and K. Krushelnick, Physical Review Letters **106**, 105002 (2011).

[58]M. Kaluza, J. Schreiber, M. Santala, G. Tsakiris, K. Eidmann, J. Meyer-ter Vehn, and K. Witte, Physical review letters **93**, 45003 (2004).

[59]R. Betti, C. D. Zhou, K. S. Anderson, L. J. Perkins, W. Theobald, and A. A. Solodov, Phys. Rev. Lett. **98**, 155001 (2007).

[60]J. Ziegler, J. Biersack, and U. Littmark, *The stopping and range of ions in matter* (Pergamon, New York, 1985).

[61]D. Hey, M. Key, A. Mackinnon, A. MacPhee, P. Patel, R. Freeman, L. Van Woerkom, and C. Castaneda, Review of Scientific Instruments **79**, 053501 (2008).

[62]C. Barty, M. Key, J. Britten, R. Beach, G. Beer, C. Brown, S. Bryan, J. Caird, T. Carlson, J. Crane, J. Dawson, A. Erlandson, D. Fittinghoff, M. Hermann, C. Hoaglan, A. Iyer, L. J. II, I. Jovanovic, A. Komashko, O. Landen, Z. Liao, W. Molander, S. Mitchell, E. Moses, N. Nielsen, H.-H. Nguyen, J. Nissen, S. Payne, D. Pennington, L. Risinger, M. Rushford, K. Skulina, M. Spaeth, B. Stuart, G. Tietbohl, and B. Wattellier, Nuclear Fusion **44**, S266 (2004).